

## High-temperature analysis of silicon properties with manganese-oxygen binary complexes

M.O. Tursunov<sup>1\*</sup> , Kh.M. Iliev<sup>2</sup>  and B.K. Ismaylov<sup>3</sup> 

<sup>1</sup>Termez State University, Termez, Uzbekistan

<sup>2</sup>Tashkent State Technical University, Tashkent, Uzbekistan

<sup>3</sup>Karakalpak State University, Nukus, Uzbekistan

\*e-mail: m.tursunov@tersu.uz

(Received December 05, 2023; received in revised form April 16, 2024; accepted May 10, 2024)

The properties of KDB-5 grade silicon, including the concentration of electroactive manganese atoms, were studied after doping with manganese using the diffusion method in the temperature range of 1100–1300 °C. It was observed that as the diffusion temperature increased within this range, the concentration of electroactive manganese atoms decreased. At 1300 °C, the concentration of these atoms became significantly lower than that of the initial boron impurity. We propose that this behavior of manganese atoms may be due to the formation of electrically neutral quasi-molecular complexes between oxygen and manganese atoms located in neighboring lattice sites. During the formation of these electrically neutral complexes, tetrahedral cells of the  $\text{Si}_2\text{O}^{++}\text{Mn}^-$  type are created within the silicon lattice. These cells slightly disturb the lattice periodicity but are significantly different in properties from the elementary silicon cell. The chemical bond in these complexes is ionic-covalent, and the binding energy of the electron differs. As the concentration of these tetrahedral cells increases, various combinations can form, potentially leading to the creation of nanocrystals of a new phase with distinct fundamental parameters.

**Key words:** silicon, manganese diffusion, oxygen, electrically neutral complex, solubility, binding energy.  
**PACS number(s):** 61.46.+w.

### 1 Introduction

As is well known, thermal and radiation defects in silicon are primarily caused by optically active oxygen atoms. Therefore, controlling the state of oxygen atoms is of significant technological interest. Studying the interaction of nickel atoms with oxygen provides a useful model, as manganese atoms in silicon have a relatively high solubility ( $N \sim 10^{18} \text{ cm}^{-3}$ ) comparable to oxygen, and are mostly in an electrically neutral state [1-2]. The formation of electrically neutral  $\text{O}^{++}\text{Mn}^-$  type in the silicon lattice. These new unit cells exhibit properties that differ significantly from those of the silicon unit cell. The chemical bonds in these new structures are ionic-covalent, and the binding energy of the electrons differs as well. As the concentration of these unit cells increases, various combinations can form, potentially leading to the creation of nanocomplexes of a new phase with distinct fundamental parameters [3-5].

### 2 Materials and methods

Single-crystal p-type silicon with a resistivity of  $\rho=5 \Omega \cdot \text{cm}$ , obtained by the Czochralski method, was used as the starting material. The oxygen concentration in the samples was  $N_{\text{O}_2}=(5\div 6) \cdot 10^{17} \text{ cm}^{-3}$ , and the dislocation density was  $S=10^3 \text{ cm}^{-2}$ . All samples underwent identical mechanical and chemical treatment. Manganese diffusion was carried out from the gas phase in evacuated quartz ampoules with a residual pressure of no more than  $P \sim 10^{-4} \text{ mm Hg}$ ; each ampoule contained two samples of both types of material [6-8]. The diffusion time ranged from  $t=0.5$  to 1 hour.

The electrical parameters of the samples were determined by the Hall effect method, and the photoelectric properties were measured using an IKS-14 installation equipped with a special cryostat. An SEM-MIRA-3 electron microscope was used for analysis. The results of the study indicated that the

samples were uniformly doped throughout their volume.

Manganese diffusion was carried out at a temperature of  $T=1300^{\circ}\text{C}$  and a diffusion time of 0.5 hours. The diffusion time was chosen in such a way as to ensure uniform doping of the samples throughout the entire volume. For all samples, the contacts were obtained by chemical nickel deposition.

### 3 Results and discession

We studied the effect of thermal annealing at specific temperatures for durations ranging from  $t=1$

to 10 hours, including oxidation in silicon (see Fig. 1). We examined the impact of thermal annealing for  $t=1$  to 10 hours on the parameters of control (initial) p-type samples with  $\rho=5 \Omega\cdot\text{cm}$  and on samples doped with Mn at  $T=1300^{\circ}\text{C}$ , which after doping had parameters close to the original. The results of these studies are presented in Figure 2. In the control (initial) samples annealed for more than  $t>5$  hours, an increase in resistivity is observed, indicating the generation of thermal donors (curve 1). Meanwhile, the electrical parameters of the manganese-doped samples remain practically unchanged (curve 2) [8-10].

Electrical parameters of the studied samples at  $T=300\text{K}$  are given in Table 1.

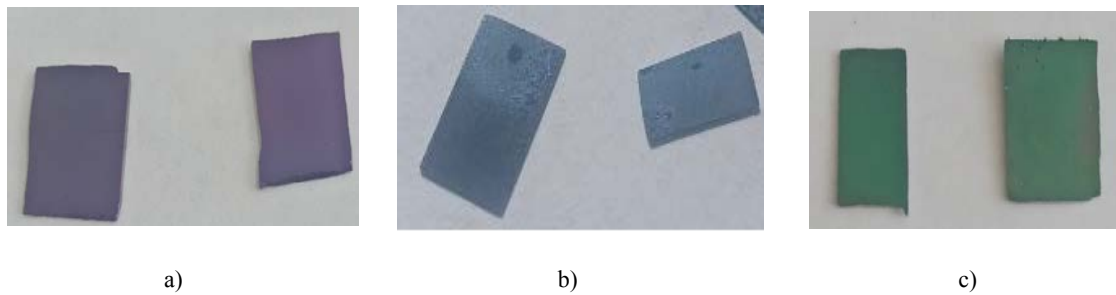


**Figure 1** – Oxidation at different temperatures in silicon: a)  $800^{\circ}\text{C}$ ; b)  $1100^{\circ}\text{C}$  and c)  $1300^{\circ}\text{C}$

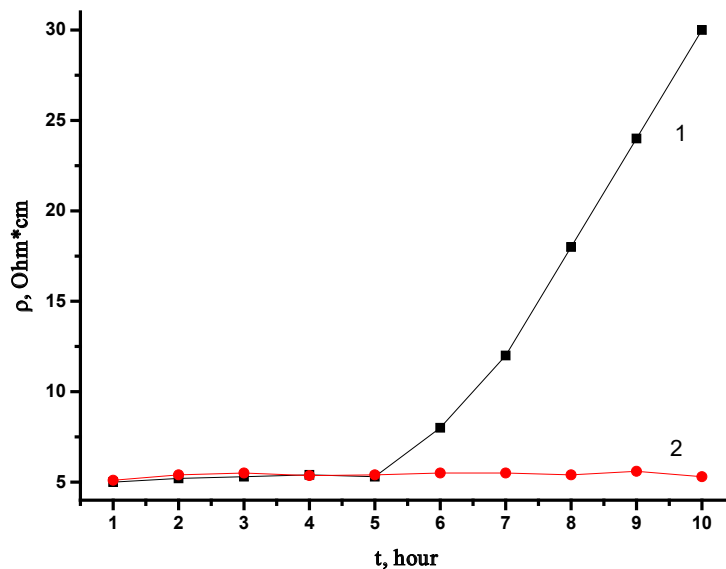


**Figure 2** – Effect of thermal annealing. 1-control (initial) samples, 2-samples alloyed with Mn at  $T = 1300^{\circ}\text{C}$

**Table 1** – Values of electrical parameters of samples after diffusion at T=1300°C (vacuum P~10<sup>-6</sup> mm Hg, rapid cooling)

Si <B,Mn>				
Conductivity type	R <sub>x</sub> , 1/Ω•cm <sup>-1</sup>	ρ, Ω•cm	μ, cm <sup>2</sup> /V•s	p, cm <sup>-3</sup>
p	1,3•10 <sup>3</sup>	5÷7	260÷270	(3,5÷3,8)10 <sup>15</sup>
Control (Si<B>)				
Conductivity type	R <sub>x</sub> , 1/Ω•cm <sup>-1</sup>	ρ, Ω•cm	μ, cm <sup>2</sup> /V•s	p, cm <sup>-3</sup>
p	1,8•10 <sup>3</sup>	5,0	360	3,5•10 <sup>15</sup>

The oxygen content (concentration of optically active interstitial oxygen atoms N<sub>O</sub><sup>opt</sup>) was assessed using IR transmission spectra in the region of 1106 cm<sup>-1</sup> (9 μm) measured on an FSM-1202 infrared spectrometer at room temperature (see Fig. 3).

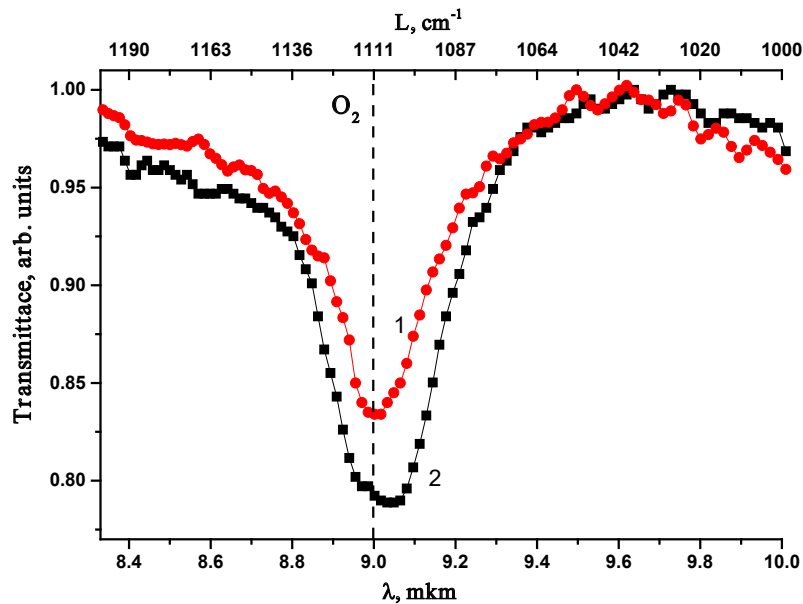


**Figure 3** – Dependence of the relative transmittance of the sample on the wavelength of the incident radiation. 1 – Si<Mn> 2 – control sample

Estimations of N<sub>O</sub><sup>opt</sup> were made using the well-known formula [11-12]:

$$N_o^{OPT} = 3.3 \cdot 10^{17} \cdot \frac{1}{d} \cdot \ln \frac{I}{I_0} \quad (1)$$

where I and I<sub>0</sub> are the intensities of incident and transmitted light, d is the thickness of the sample.

Using formula (1), we determined the concentration of optically active oxygen in silicon for the manganese-doped and control samples. Then we have:

1. Si < Mn >

$$N_o^{OPT} = 3.3 \cdot 10^{17} \cdot \frac{1}{d} \cdot \ln \frac{I}{I_0} = 2.5 \cdot 10^{17} \text{ cm}^{-3}$$

2. Si < control >

$$N_o^{OPT} = 3.3 \cdot 10^{17} \cdot \frac{1}{d} \cdot \ln \frac{I}{I_0} = 5.4 \cdot 10^{17} \text{ cm}^{-3}$$

$$3. N_o^{opt(control)} - N_o^{opt(Mn)} = 5.4 \cdot 10^{17} - 2.5 \cdot 10^{17} = 2.9 \cdot 10^{17} \text{ cm}^{-3}$$

The results show that the oxygen concentration decreases by a factor of 2.16. Therefore, it can be assumed that doping with manganese significantly reduces the amount of optically active oxygen.

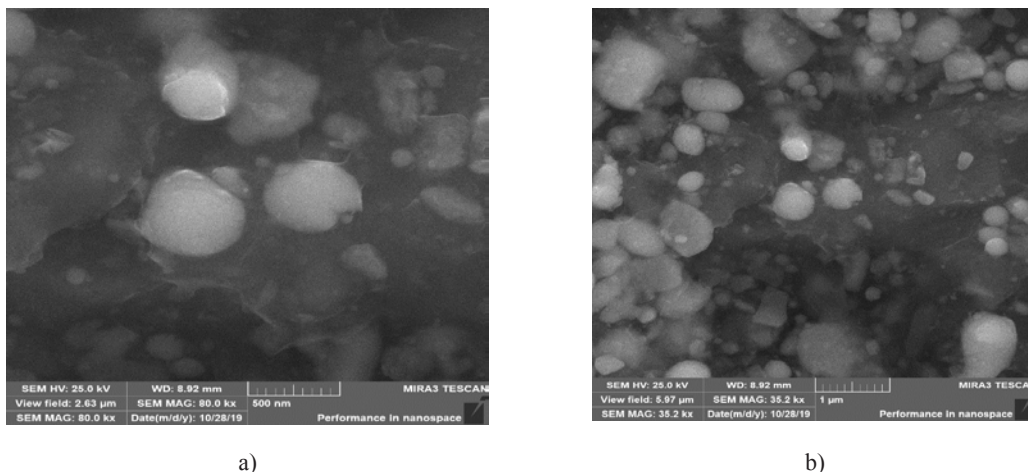


**Figure 4** – Electron diffraction patterns "for reflection" from a single-crystalline film of manganese oxide on silicon: a) at a resolution of 500 nm; b) at a resolution of 1  $\mu\text{m}$

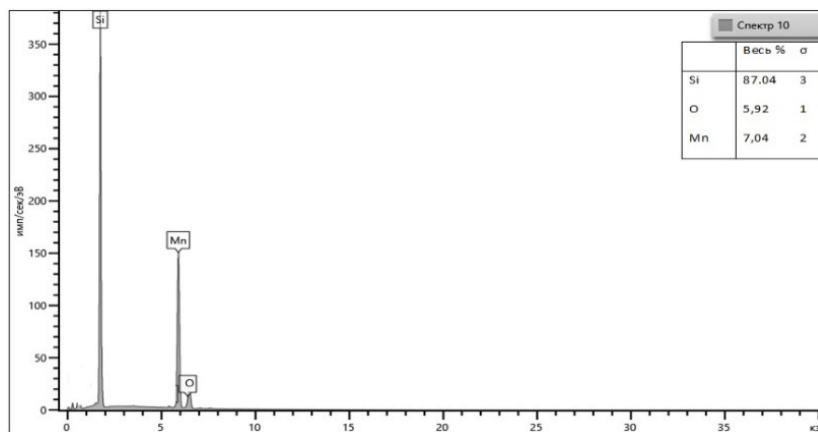


**Figure 5** – Electron diffraction patterns "for reflection" from a single-crystalline film of manganese and oxygen on silicon

#### 4 Consideration of the possible structures of manganese-oxygen complexes.

From a formal perspective, such formations can have the composition  $\text{Si}_k\text{Mn}^m\text{O}^n$ , where the value of  $k$  is determined by the need to integrate the complex into the tetrahedral silicon lattice, with different possible charge states for all atoms. In this scenario, the requirements of tetrahedral coordination of surrounding bonds within the lattice, the absence of mechanical stress, and the presence of electronic configurations in the constituent atoms that ensure stable chemical bonding must be met.

In the simplest case, where  $m=n=1$ , the manganese-oxygen complex can formally adopt structures such as  $\text{Mn}^{+2}\text{O}^{-2}$ ,  $\text{Mn}^{+1}\text{O}^{-1}$ ,  $\text{Mn}^0\text{O}^0$ ,  $\text{Mn}^{-1}\text{O}^{+1}$  and  $\text{Mn}^{-2}\text{O}^{+2}$ , supplemented with the required

number of silicon atoms ( $k$ ) to complete the lattice [13-15].

It is particularly important to emphasize that in such complexes, the conventional concepts of atomic valence and electronegativity may be altered. This is because the complex is not an isolated manganese-oxygen molecule or a crystal of such molecules, but rather a part of the silicon crystal lattice. Consequently, the system must achieve a minimum of free energy within the silicon lattice environment. The presence of the silicon lattice imposes additional requirements on the structure of the complexes: tetrahedral coordination of surrounding bonds within the lattice, absence of significant mechanical stress, and appropriate electronic configurations of the constituent atoms to ensure stable chemical bonds both within and around the complex.

1. *Structure of  $Mn^{+2}O^{-2}$* . The bond between atoms is ionic, consistent with their electronegativity values. This structure aligns with traditional concepts of the chemical bond between oxygen and metals. The sum of the ionic radii of  $O^{-2}$  (0.14 nm) and  $Mn^{+2}$  (0.083 nm) totaling 0.223 nm, closely matches the two covalent radii of silicon ( $2 \times 0.111$  nm), preventing lattice stress. However, the oxygen atom, with a fully completed (inert) outer shell, cannot effectively interact with the surrounding three silicon atoms, breaking these bonds. Even if two silicon bonds are closed to a neighbor, one broken bond remains, potentially detaching an electron and exhibiting electrical activity. Manganese in the  $Mn^{+2}$  state also has a stable outer shell, posing similar issues with external lattice bonds.

2. *Structure of  $Mn^{+1}O^{-1}$* . The bond between atoms is ionic, matching their electronegativity. The oxygen atom, with an incompletely filled (7-electron) outer shell, can interact effectively with one silicon atom, forming an oxygen-silicon ionic bond, while the other two bonds break. If two silicon bonds are closed to a neighbor, oxygen's electrical activity is absent. Manganese in the  $Mn^{+1}$  state also has one weakly bound electron and can form an ionic bond with one silicon atom, breaking the other two bonds. If two silicon bonds close to a neighbor, manganese's electrical activity is also absent.

3. *Structure of  $Mn^0O^0$* . The bond between atoms is potentially covalent, not matching their electronegativity values. In this case, the oxygen atom, with an incompletely filled (6-electron) outer shell, should exhibit acceptor properties towards surrounding silicon atoms. Manganese in the  $Mn^0$  state also lacks a stable outer shell, leading to issues with external bonds.

4. *Structure  $Mn^{-1}O^{+1}$* . The bond between atoms is ionic, not consistent with their electronegativity values. The oxygen atom, with an incompletely filled (5-electron) outer shell, can interact effectively with three silicon atoms, similar to a covalent bond, leaving two excess oxygen electrons that could create electrical activity. Manganese in the  $Mn^{-1}$  state also lacks a stable outer shell, introducing the possibility of electrical activity.

5. *Structure of  $Mn^{-2}O^{+2}$* . The bond between atoms is ionic, not matching their electronegativity values. The oxygen atom, with an incompletely filled (4-electron) outer shell, can interact effectively with three silicon atoms and manganese, forming an ionic-covalent bond. This configuration should avoid electrical activity. Manganese in the  $Mn^{-2}$  state also

has a 4-electron outer shell, allowing tetrahedral covalent bonds with neighbors without causing electrical activity.

The structure of site complexes between Mn atoms and Group VI elements in the silicon lattice is shown in Fig. 6. The distance between the atoms included in the complex differs slightly from the silicon-silicon distance in the lattice, since impurities during the formation of complexes are in site positions and are held in these positions by covalent bonds. Then distance = 2.27 Å.

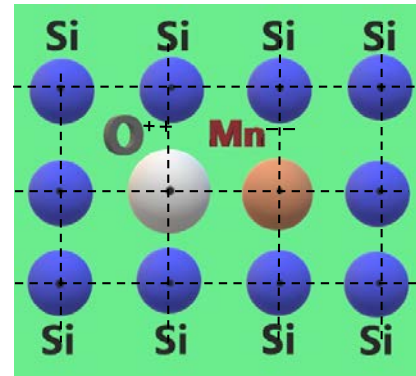


Figure 6 – Structure of site complexes between Mn atoms and Group VI elements in the silicon lattice

Calculated binding energy based on experimental results.

1)  $Si < MnO >$  dielectric constant of the interaction medium (silicon lattice) = 12. Considering the impurity-impurity bond to be ionic and taking the charge multiplicity equal to unity, we can estimate the force of attraction between the oxygen and manganese atoms [16-18]:

$$F_{MnO} = \frac{4kq^2}{\epsilon r_l^2} = 1,49 \cdot 10^{-9} \quad (2)$$

Where:  $q = 1.6 \cdot 10^{-19}$  C – electron charge, coefficient  $k = 9 \cdot 10^9 \frac{N \cdot m^2}{C^2}$

Then the minimum value of the binding energy between atoms in the complex can be estimated by the expression:

$$E_{MnO} = Fr_l = 1,49 \cdot 10^{-9} \cdot 2.34 \cdot 10^{-10} = 3,48 \cdot 10^{-19} J = 2.17 eV \quad (3)$$

$$2) \text{ For Si<MnS>} \\ \varepsilon = 12, r_l = 2,73 \text{ \AA}, q = 1.6 \cdot 10^{-19} \text{ C}, \\ k = 9 \cdot 10^9 \frac{N \cdot m^2}{C^2}; F_{MnS} = \frac{4kq^2}{\varepsilon r_l^2} = 1,03 \cdot 10^{-9} \quad (4)$$

$$E_{MnS} = Fr_l = 1,03 \cdot 10^{-9} \cdot 2,34 \cdot 10^{-10} = \\ = 2.41 \cdot 10^{-19} \text{ J} = 1,5 \text{ eV} \quad (5)$$

$$3) \text{ For Si<MnSe>} \\ \varepsilon = 12, r_l = 2,84 \text{ \AA}, q = 1.6 \cdot 10^{-19} \text{ C}, \\ k = 9 \cdot 10^9 \frac{N \cdot m^2}{C^2};$$

$$F_{MnSe} = \frac{4kq^2}{\varepsilon r_l^2} = 9,52 \cdot 10^{-10} \quad (6)$$

$$E_{MnSe} = Fr_l = 9,52 \cdot 10^{-10} \cdot 2,34 \cdot 10^{-10} = \\ = 2.2 \cdot 10^{-19} \text{ J} = 1,39 \text{ eV} \quad (7)$$

4) Si&lt;MnTe&gt;

$$\varepsilon = 12, r_l = 3.01 \text{ \AA}, q = 1.6 \cdot 10^{-19} \text{ C}, \\ k = 9 \cdot 10^9 \frac{N \cdot m^2}{C^2}; F_{MnTe} = \frac{4kq^2}{\varepsilon r_l^2} = 8.5 \cdot 10^{-10} \quad (8)$$

$$E_{MnTe} = Fr_l = 8.5 \cdot 10^{-10} \cdot 2.34 \cdot 10^{-10} = \\ = 1.98 \cdot 10^{-19} \text{ J} = 1,24 \text{ eV} \quad (9)$$

$$E_{MnO} \sim 2,17 > E_{MnS} \sim 1,5 > E_{MnSe} \sim 1,39 > E_{MnTe} \sim 1,24$$

The concentrations of Mn impurity atoms, group VI elements and their complexes are shown in Table 3 [19-20].

**Table 2** – Binding energies between Mn atoms and Group VI elements in the silicon lattice, calculated from the Coulomb interaction

Binary complexes	Minimum binding energy $E$ , eV
Si <sub>2</sub> O <sup>++</sup> Mn <sup>-</sup>	2,17
Si <sub>2</sub> S <sup>++</sup> Mn <sup>-</sup>	1,5
Si <sub>2</sub> Se <sup>++</sup> Mn <sup>-</sup>	1,39
Si <sub>2</sub> Te <sup>++</sup> Mn <sup>-</sup>	1,24

**Table 3** – Concentrations of impurity Mn atoms, group VI elements and their complexes

$t, ^\circ\text{C}$	$C_{Mn}, \text{cm}^{-3}$	$C_O, \text{cm}^{-3}$	$C_{MnO}, \text{cm}^{-3}$	$N_s, \text{cm}^{-3}$
1300	$2 \cdot 10^{16}$	$5 \cdot 10^{17}$	$4 \cdot 10^{16}$	$5 \cdot 10^{22}$
$t, ^\circ\text{C}$	$C_{Mn}, \text{cm}^{-3}$	$C_S, \text{cm}^{-3}$	$C_{MnS}, \text{cm}^{-3}$	$N_s, \text{cm}^{-3}$
1100	$1,5 \cdot 10^{16}$	$5 \cdot 10^{16}$	$4 \cdot 10^{15}$	$3 \cdot 10^{22}$
$t, ^\circ\text{C}$	$C_{Mn}, \text{cm}^{-3}$	$C_{Se}, \text{cm}^{-3}$	$C_{MnSe}, \text{cm}^{-3}$	$N_s, \text{cm}^{-3}$
1250	$2 \cdot 10^{16}$	$1 \cdot 10^{17}$	$1 \cdot 10^{15}$	$2,5 \cdot 10^{22}$
$t, ^\circ\text{C}$	$C_{Mn}, \text{cm}^{-3}$	$C_{Te}, \text{cm}^{-3}$	$C_{MnTe}, \text{cm}^{-3}$	$N_s, \text{cm}^{-3}$
1250	$2 \cdot 10^{16}$	$5 \cdot 10^{17}$	$1 \cdot 10^{15}$	$2,5 \cdot 10^{22}$

In this table:

$T$  – complexation temperature for complex formation Si<sub>2</sub>Mn<sup>-</sup>B<sup>VI++</sup>.

$C_{Mn}$  – solubility of manganese at a given diffusion temperature.

$C_O$  – solubility of group VI elements at a given diffusion temperature.

$C_{MnO}$  – concentration of complexes of group VI elements and manganese.

$N_s$  – atomic concentration.

Using the Arrhenius equation written for the equilibrium between complexes and individual impurity atoms at temperature  $T$ , we can write [21-22]



$$\frac{d \ln \alpha}{dT} = \frac{E_a}{RT^2} \quad (10)$$

$$E_{\text{MnO}} \sim 1,46 \text{ eV} > E_{\text{MnS}} \sim 1,24 \text{ eV} > E_{\text{MnSe}} \sim 1,09 \text{ eV} > E_{\text{MnTe}} \sim 0,87 \text{ eV}$$

$$E_a = kT \ln \left( \frac{N \cdot C_{AB}}{4C_A C_B} \right) \quad (11)$$

It should be noted that the binding energy in complexes decreases with increasing sizes of Group VI element atoms.

**Table 4** – Binding energies between Mn atoms and Group VI elements in the silicon lattice, calculated using the Arrhenius equation

Binary complexes	Binding energy, $E$ , eV
$\text{Si}_2\text{O}^{++}\text{Mn}^-$	1,46
$\text{Si}_2\text{S}^{++}\text{Mn}^-$	1,24
$\text{Si}_2\text{Se}^{++}\text{Mn}^-$	1,09
$\text{Si}_2\text{Te}^{++}\text{Mn}^-$	0,87

The patterns of decreased binding energy in complexes involving Mn and Group VI elements (O, S, Se, Te), as calculated from Coulomb interactions, align with the Gibbs energy trends [23-25]. Additionally, the calculated binding energies, using experimental values for the concentration of impurities and complexes, confirm this decrease in binding energy. From the analysis of experimental data and numerical calculations, we can conclude that the physical model of complex formation between manganese and Group VI element atoms is generally accurate.

## 5 Conclusions

Based on the results obtained, we propose a model for the formation of electrically neutral molecules resulting from the interaction between manganese and oxygen atoms. This model considers both lattice site and interstitial arrangements of manganese and oxygen atoms. The resulting silicon material contains a relatively high concentration  $N \sim (3 \div 4) \cdot 10^{16} \text{ cm}^{-3}$  of tetrahedral cells of the  $\text{Si}_2\text{O}^{++}\text{Mn}^-$  type in the silicon lattice, which is of significant scientific and practical interest.

Research into methods to increase the concentration of these binary cells and explore their properties could pave the way for creating a new class of silicon-based materials for optoelectronic and

photoelectric devices. Silicon enriched with binary cells of the  $\text{Si}_2\text{Mn}^- \text{B}^{\text{VI}++}$  type holds the potential to facilitate the development of innovative optoelectronic and nanoelectronic devices, as well as highly efficient silicon-based solar cells with parameters comparable to or better than those of expensive multi-stage photocells based on AIIIBV materials.

The diffusion conditions allow for a significant increase in the concentration of electroactive manganese atoms, thereby enhancing the described phenomena and expanding the functionality of manganese-doped silicon in optoelectronics and spintronics. Consequently, developing technology to boost the concentration of these binary cells in silicon is of great scientific and practical interest. This advancement could lead to the future creation of a new class of silicon-based materials for optoelectronic and photoelectric devices.

## Acknowledgements

The work was financially supported by the Ministry of Innovative Development of the Republic of Uzbekistan within the framework of the project F-OT-2021-497 – “Development of the scientific foundations for the creation of solar cogeneration plants based on photovoltaic thermal batteries”.

## References

1. Milvidsky M.G., Chaldyshev V.V. Nanosized atomic clusters in semiconductors – a new approach to the formation of material properties // *Physics and technology of semiconductors*. – 1998. – Vol. 32. – no. 5. – P. 513-522. <https://doi.org/10.1134/1.1187418>
2. Zainobiddinov S. Physical foundations of the formation of deep levels in silicon // *Tashkent, Fan* – 1984. – P. 160.
3. Boltaks B.I. Diffusion and point defects in semiconductors // *Science, Leningrad* – 1972. – P. 384.
4. Boltaks B.I., Bakhadirkanov M.K., Gorodetsky S.M., Kulikov G.S. Compensated silicon // *Leningrad, Nauka* – 1972. – P. 122.
5. Bakhadyrkhanov M.K., Isamov S.B., Zikrillayev N.F., Tursunov M.O. Anomalous photoelectric phenomena in silicon with nanoclusters of manganese atoms // *Semiconductors*. – 2021. Vol. 55. – No. 6. – P. 636–639. <https://doi.org/10.1134/s1063782621060038>
6. Ismailov K.A., Iliev X.M., Tursunov M.O., Ismaylov B.K. Formation of complexes consisting of impurity Mn atoms and group VI elements in the crystal lattice of silicon. // *Semiconductor Physics, Quantum Electronics & Optoelectronics*. – 2021. – Vol. 24. – No. 3. – P. 255–260. <http://dx.doi.org/10.15407/spqeo24.03.255>
7. Ismailov, K.A., Kenzhaev, Z.T., Koveshnikov, S.V., Kosbergenov, E.Z., Ismaylov, B.K. Radiation Stability of nickel doped solar cells // *Physics of the Solid State*. – 2022. – Vol. 64(3). – P. 154–156. <https://doi.org/10.1134/S1063783422040011>
8. Zikrillayev, N.F., Mavlonov, G.Kh., Trabzon, L., Koveshnikov S.V., Kenzhaev Z.T., Ismailov, T.B., Abduganiev, Y.A., Magnetic properties of silicon with paramagnetic impurity atoms // *East European Journal of Physics*. – 2023. Vol.15(6). – P. 380–384. [http://dx.doi.org/10.21272/jnep.15\(6\).06001](http://dx.doi.org/10.21272/jnep.15(6).06001)
9. Ismaylov, B.K., Zikrillayev, N.F., Ismailov, K.A., Kenzhaev, Z.T. Clusters of impurity nickel atoms and their migration in the crystal lattice of silicon // *Physical Sciences and Technology* – 2023. – Vol.10(1). – P. 13–18; <https://doi.org/10.26577/phst.2023.v10.i1.02>
10. Zikrillayev, N.F., Isamov, S.B., Koveshnikov, S.V., Kenzhaev, Z.T., Turekeev, K.S. Codiffusion of gallium and phosphorus atoms in silicon // *Surface Engineering and Applied Electrochemistry*.- 2023. – Vol.59(2).- P. 210–215. <https://doi.org/10.3103/S1068375523020199>
11. M.K. Bakhadirkanov, Kh.M. Iliev, M.O. Tursunov, S.B. Isamov, S.V. Koveshnikov, M.Kh. Majitov. Electrical properties of silicon doped with manganese via high-temperature diffusion // *Inorganic Materials* – 2021. – Vol. 57. – No. 7. – P. 655-662. <https://doi.org/10.1134/S0020168521070013>
12. Nakashima H., Hashimoto K. Deep impurity levels and diffusion coefficient of manganese in silicon // *J. Appl. Phys.* – 1991. – Vol. 69. – № 3 – P. 1440-1445. <https://doi.org/10.1063/1.347285>
13. Bakhadyrkhanov, M.K., Kenzhaev, Z.T. Optimal conditions for nickel doping to improve the efficiency of silicon photoelectric cells // *Technical Physics*. – 2021. – Vol. 66(7). P. 851–856. <https://doi.org/10.21883/JTF.2021.06.50868.332-20>
14. Bakhadyrkhanov, M.K., Isamov, S.B., Kenzhaev, Z.T., Koveshnikov, S.V. Studying the effect of doping with nickel on silicon-based solar cells with a deep p–n-junction // *Technical Physics Letters*.- 2019.- Vol. 45(10). P. 959–962. <http://dx.doi.org/10.1134/S1063785019100031>
15. Bakhadyrkhanov, M.K., Isamov, S.B., Kenzhaev, Z.T., Melebaev D., Zikrillayev, Kh.F., Ikhtiyarova, G.A. Silicon photovoltaic cells with deep p–n-junction // *Applied Solar Energy (English translation of *Geliotekhnika*)*. – 2020.- Vol. 56(1).- P. 13–17. <https://doi.org/10.3103/S0003701X2001003X>
16. Bakhadyrkhanov M.K., Iliev Kh.M., Sattorov O.E., Ismailov K.A., Saparniyazova Z.M., Norkulov N., Asanov D. Zh. Interaction between multiply charged manganese nanoclusters and sulfur atoms in silicon // *Inorganic Materials*. – 2012. – V.48. – № 3. – P.325-328. <http://dx.doi.org/10.1134/S0020168515070031>
17. Zainabidinov, S.Z., Musayev, K.N., Turgunov, N.A. et al. Dopant micro association mechanisms in Si ⟨Mn⟩ and Si ⟨Ni⟩ // *Inorganic Materials*. – 2012. – V.48. – P. 1065–1069. <https://doi.org/10.1134/S0020168512110192>
18. Bakhadyrkhanov, M.K., Kenzhaev, Z.T., Koveshnikov, S.V., Usmonov, A.A., Mavlonov, G.K. Formation of complexes of phosphorus and boron impurity atoms in silicon // *Inorganic Materials*. – 2022. Vol. 58(1). <https://doi.org/10.1134/S0020168522010034>
19. Taskin A.A., Tishkovsky E.G. Formation of complexes associated with selenium atoms in silicon // *Physics and Technology of Semiconductors*. – 2002. Vol. 36(6), P. 641-649. <https://doi.org/10.1134/1.1485656>
20. Iliev Kh.M., Tursunov M.O., Koveshnikov S.V., Khudaynazarov Z.B. Research of properties of silicon with binary nanoclusters with participation of Mn and Se atoms // *Semiconductor Physics and Microelectronics*. – 2020. – Vol. 2. – Is 2. – P. 59-62. <https://doi.org/10.5281/zenodo.100096>
21. Weixin Ouyang, Feng Teng, Jr-Hau He, Xiaosheng Fang. Enhancing the photoelectric performance of photodetectors based on metal oxide semiconductors by charge-carrier engineering // *Adv. Funct. Mater.* – 2019. – Vol.29(9). <http://dx.doi.org/10.1002/adfm.201807672>
22. R. Mainz, A. Singh, S. Levchenko, M. Klaus, C. Genzel, K.M. Ryan, T. Phase-transition-driven growth of compound semiconductor crystals from ordered metastable nanorods // *Nature Communications*. – 2014. – Vol. 3133. <https://doi.org/10.1038/ncomms4133>
23. Bakhadyrkhanov M.K., Askarov Sh.I, and Norkulov N. Some features of chemical interaction between a fast diffusing impurity and a group VI element in silicon. // *Physics state solid*. – 1994. – No. 142. – P. 339-346. <https://doi.org/10.1002/pssa.2211420206>
24. Glushko V.P. Thermodynamic constant for materials // *Issue. 7 – Pt 1, Nauka, Moscow* -1974.
25. Björk M. T., Schmid H., Knoch J., Riel H., Riess W. Donor deactivation in silicon nanostructures // *Nature Nanotechnology*.- 2009. -Vol. 4. – P. 103-107. <https://doi.org/10.1038/nnano.2008.400>



**Information about authors:**

*Tursunov Mamasobir Ochildiyevich (corresponding author), PhD in physical and mathematical sciences, is an Associate professor at Termez State University, (Termez, Uzbekistan) e-mail: mtursunov@tersu.uz;*

*Iliev Khalmurat Midzhitovich, Doctor of Physical and Mathematical Sciences, is a Professor at Tashkent State Technical University (Tashkent, Uzbekistan) e-mail: xolmurodov.iliev@tdtu.uz;*

*Ismaylov Bayrambay Kanatbaevich, PhD in physical and mathematical sciences, is a DSc student at Karakalpak State University (Nukus, Uzbekistan) e-mail: i.bairam@bk.ru*